Scaling laws in etched Si surfaces

Marta E. R. Dotto and Maurício U. Kleinke*
NanoStructures and Interfaces Laboratory, DFA/IFGW/UNICAMP, CP 6165, CEP 13081-970, Campinas, SP, Brazil
(Received 26 April 2002; published 21 June 2002)

Self-affine scaling behavior of etched crystalline Si surfaces has been investigated by atomic force microscope. Si surfaces were etched by a small drop (a few μL) of NaOH solution. Percolation characteristics were observed at the initial stages of Si(100) chemical etching. Roughness exponent (α) values increase with etching time, from 0.6 to 0.8, and the α functional behavior with respect to the etching power agrees with the Kessler-Levine-Tu model. Anomalous scaling behavior was characterized for etched Si(111) surfaces. The local value of the roughness exponent is associated to the diffusional process of plateau growth. The global value of α is close to 0.4, a typical value for the Kardar-Parisi-Zang model, reflecting the highest growth rates on surfaces with higher slopes.

DOI: 10.1103/PhysRevB.65.245323 PACS number(s): 68.35.Bs, 68.35.Ct, 68.35.Rh

I. INTRODUCTION

The chemical treatment of clean silicon wafer surfaces generally involves HF etching.[1] Industrial crystalline Si wafers can present dislocations or steps on vicinal terraces, and these surface defects can be disclosed by a salt solution bath. Silicon etching rate is a function of crystalline orientation, doping, etching solution and stirring.[2]

Since the development of the atomic force microscope (AFM) this nondestructive technique has been used to obtain three-dimensional images that can be characterized by a fractal approach such as scaling laws.[3] In the last few years surfaces were extensively studied using scaling concepts.[4–6] However, only a few papers discuss self-affine scaling during surface growth generated by a chemical etching process.[7,8]

For the same chemical conditions (concentration and temperature of solution, solvent class, etc.) the experimental apparatus design (geometric characteristics, gas flow, solution stirring, etc.) plays a fundamental role in the etched surface growth dynamics. During the chemical etching, the solution can be stirred by natural convection (density and/or temperature gradients) or forced convection (jet or ultrasonic bath). A less common type of natural stirring is that resultant from the Marangoni effect,[9] where two fluids in contact present interfacial tension gradient, and this gradient is the driving force to promote the fluid transport.

Recently we studied the scaling behavior of chemical etched Si surface by AFM.[10] Si surfaces were etched at distinct experimental conditions: sample immersed in quiescent solution, sample immersed in solution under ultrasonic stirring or etched by a small drop of solution. During the attack, these distinct experimental apparatuses modify the mass transport. Consequently, the corrosion front velocity and the surface growth dynamics are also modified. The functional behavior of roughness exponents with respect to the corrosion front velocity agrees with the Kessler-Levine-Tu model.[11]

Santra and Sapoval[7] proposed a model for attack of solids by chemical solutions. In their model, the etching rate is a randomic function, independent of the etching time or the sample environment. They assume a finite number of etchant molecules initially in contact with the surface, and a decreasing etching rate with the decrease of the number of etchant molecules. At the end of the etching process, the interfacial structure becomes very irregular, with a pattern similar to the one observed at a percolation threshold.

R. Cafieiro[8] presented a model for chemical etching of crystalline silicon ($1d+1$ dimension) with a local anisotropy factor. The model discusses the intrinsic anisotropy of the etching rate, and proposes a local dynamics connected to the global equilibrium. The anisotropy factor is related to the ratio $v(111)/v(100)$, where $v(111)$ and $v(100)$ are the etching rate at the corresponding crystallographic direction. The roughness exponent varies from 0.63 (nonanisotropic system) to 0.93 (completely anisotropic system). The experimental results[8] suggest that the agitation increases and the etchant concentration decreases the anisotropic etching rate.

Kasparian *et al.*[2] discussed the anisotropic etching of Si(111) by NaOH at the atomic level. The first steps of the etching process were simulated using a Monte Carlo method and measured in real time by scanning tunneling microscope (STM). The etched Si surface observed by STM showed the growth of triangles, for short etching times (a few minutes).

In our work, crystalline Si wafers were etched by a small drop of NaOH. The small drop increases the concentration gradient, generating interfacial turbulence near the surface.[12,13] Etched Si surface images were obtained by AFM, and these images were treated to evaluate the dynamic, growth, and roughness scaling exponents values.

II. MATERIAL AND METHODS

A. Sample preparation and AFM analysis

Polished Si(100) (n doped, 0.02 Ω cm) and Si(111) (p doped, 7 Ω cm) from Virginia INC, with misalignment $<0.2°$, were used. The samples (1×1 cm) were previously deoxidized for $\sim$1 min in HF solution and rinsed with bidistilled water. A 1-M NaOH solution microdrop was deposited on the deoxidized surface. The microdrop volume was 5 μL [Si(100)] and 1 μL [Si(111)]. The etching time was varied from 3 to 160 min, at a temperature of $(23\pm2)°$C. During the etching, the sample and the etchant drop were kept in saturated aqueous ambient (sa), or in nonsaturated aqueous ambient ($\approx$50% humidity) (nsa). After a final rinse with bi-

distilled water, the sample was dried under nitrogen flow and stored in vacuum (10^{-2} Torr).

The images were obtained with a Topometrix TMX 2000 SPM operating in the contact AFM mode. Some samples of Si(111) sa were observed by an AutoProbe CP Research SPM, from ThermoMicroscopes, operating at similar conditions. Tips of high aspect ratio (Microlever tip, radius <20 nm and angle $\sim 20°$, from ThermoMicroscopes) were used, in order to minimize the convolution effects. All images (300 $\times$300 pixel for Topometrix and 512$\times$512 pixel for AutoProbe CP Research) were acquired with a 2-Hz scan frequency. Image scan length was varied from 200 nm to 7 μm.

B. Statistical treatment of images

The height-height correlation function (HHC) is one of the most convenient correlation functions to characterize experimental self-affine surfaces. HHC is defined as

$$\mathrm{HHC}(r,t)=\langle |h(r-r')-h(r')|^2\rangle^{1/2}, \tag{1}$$

where $h(r')$ is the surface height at position r', $h(r-r')$ is the surface height at the circle with radius r centered at r' and $\langle \ldots \rangle$ means averaging over all images at time t. For an arbitrary self-affine surface, HHC scales with r as HHC $\sim r^{\alpha}$ where α is the roughness exponent.[14]

To characterize the scaling behavior of surfaces using AFM it is necessary to have an image set with image sizes varying a few orders of magnitude. Larger images present maximum values for r (r_{max}) and for HHC (HHC_{max}). If the surface presents self-affine behavior, $r\sim b r_{max}$ and HHC $\sim b^{\alpha}\mathrm{HHC}_{max}$. Using the maximum values, we have

$$\ln[\mathrm{HHC}(r,t)]\sim \alpha \ln(r)+\ln\left(\frac{\mathrm{HHC}_{max}}{r_{max}^{\alpha}}\right), \tag{2}$$

where α is the slope in a log-log plot of HHC vs r. If the sample presents a perfectly self-affine behavior, the HHC curves for distinct images will collapse, and the $\ln(\mathrm{HHC}_{max}/r_{max}^{\alpha})$ term remains constant. This term is related to the image bumps or mounds. The vertical displacement on the HHC curves obtained from images with distinct sizes can be related to the disappearance of these bumps from images acquired at small scan size.

Another important parameter to describe the interface growth dynamics is the surface width $[w(t)]$ (or *-root-mean-square* roughness):

$$w(t)=(\langle h^2\rangle-\langle h\rangle^2)^{1/2}, \tag{3}$$

where h is the surface height at point on the $l\times l$ image matrix at time t. Surface width represents a correlation length perpendicular to the surface ($\xi_{\perp}$) and scales with time as $w(t)\sim t^{\beta}$ where β is the growth exponent.[15] The correlation length parallel to the surface ($\xi_{\parallel}$) scales with time as $\xi_{\parallel}\sim t^{1/Z}$, where Z is the dynamic exponent ($Z=\alpha/\beta$).[15]

To increase the critical exponents' evaluation accuracy, a set of images spanning several orders of magnitude were acquired for each analyzed region. AFM images were treated by a program using a mixed technique, based on the multiple-image and a single-image variography, described elsewhere.[16]

One of the most useful technique to characterize a percolation process on a surface is to intersect the image by an horizontal ''sea'' plane producing ''islands.''[17] When these islands aggregate, they form a percolation network. Scanning probe microscope results involving percolation were described for discontinuous films[18] or for conductor-insulator composites.[19] Buzio *et al.*[20] measured films of carbon clusters by AFM. They suggest that the local surface defects present common aspects with the quenched noise at the percolation system. For our image sets the sea level was chosen at 40% of the maximum surface height. The ramified nature of percolation clusters results in a perimeter (P) that scales linearly with area (A) for large clusters,[17] $P\sim A^{\phi}$.

C. Models for surface growth

Several models can be used to describe the growth dynamics.[15] We shall be interested in models in $2d+1$ dimensions. One of the simplest is the Wolf-Villain model (WV), which is a linear diffusive model:[21]

$$\frac{\partial h}{\partial t}=R_D-\nu\nabla^4 h+\eta, \tag{4}$$

where R_D is the deposition rate, ν is a constant, η is a roughening term with stochastic characteristics of a fluctuation process, and the $-\nu\nabla^4 h$ term accounts for smoothening by surface diffusion. Values of roughness, growth, and dynamic exponents obtained from this model are 1, 1/4, and 4, respectively.

One attempt to make surface diffusion a conserved quantity is to add a nonlinear term to Eq. (4) which results in the Lai–Das Sarma–Villain (LDV) equation:[22]

$$\frac{\partial h}{\partial t}=R_D-\nu\nabla^4 h+\lambda\nabla^2(\nabla h)^2+\eta, \tag{5}$$

where λ is a constant and $\lambda\nabla^2(\nabla h)^2$ is the nonlinear term that models the fact that steps can act as a source or sink of atoms on a growing surface. The scaling exponent values for the LDV model are $\alpha\cong 2/3$, $\beta\cong 1/5$, and $Z\cong 10/3$.[22]

López[23] discussed the presence of anomalous surface roughness in the LDV equation [Eq. (5)]. Anomalous surface roughness is characterized by distinct scaling relations for the local and the global surface fluctuations, with a crossover length delimitating the local and the global regions. For $1d+1$ dimensions, the LDV model presents a local roughness exponent $\alpha_{local}\cong 0.7$.[24]

A typical nonlinear model for interface growth is the Kardar-Parisi-Zhang (KPZ) model:[25]

$$\frac{\partial h}{\partial t}=R_D+\nu\nabla^2 h+\frac{\lambda}{2}(\nabla h)^2+\eta, \tag{6}$$

where the $\nu\nabla^2 h$ term is the surface tension term, as it tends to smooth the interface. The nonlinear $(\lambda/2)(\nabla h)^2$ term accounts for growth along the normal direction (lateral growth).[6] The corresponding scaling exponents are $\alpha\cong 0.39$,

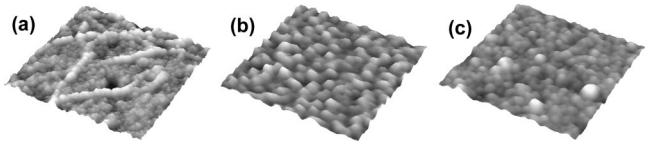

FIG. 1. AFM images of etched Si(100) surface in sa: (a) 2.5 μm$\times$2.5 μm$\times$93 nm, $t=20$ min; (b) 3.5 μm$\times$3.5 μm$\times$121 nm, $t=50$ min; and (c) 5 μm$\times$5 μm$\times$137 nm, $t=110$ min.

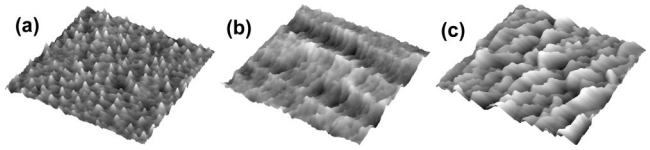

FIG. 2. AFM images of etched Si(111) surface in nsa: (a) 2 μm$\times$2 μm$\times$6 nm, $t=3$ min; (b) 3 μm$\times$3 μm$\times$13 nm, $t=40$ min; and (c) 5 μm$\times$5 μm$\times$54 nm, $t=110$ min.

$\beta\cong0.24$, and $Z\cong1.61$. A great number of experiments can be described by the KPZ model. However, this description can be applied only to uncorrelated noise systems.

Many experiments present quenched noise, i.e., the irregularities in the domain of experimental conditions are fixed during the essay. For these systems Kessler, Levine, and Tu proposed modifications on the KPZ model [Eq. (6)]. The KLT model[11] describes a fluid interface moving through a random medium:

$$\frac{\partial h}{\partial t}=F+\nu\nabla^2 h+\eta(\vec{x},t), \tag{7}$$

where F is the pushing force applied to a piston in order to compress the fluid and $\eta(\vec{x},t)$ represents the quenched noise. This model is typical for percolation processes, and the α value (evaluated at the propagation front) is a function of the piston velocity, varying from 0.93 (low velocities) to 0.55 (high velocities).[11]

D. Etching of Si by NaOH

The Si etching by NaOH was described by Rappich.[26] Initially, surface Si atoms are passivated by hydrogen, forming Si-H bonds. Hydrolysis of Si-H bonds followed by a fast consecutive hydrolysis of the Si-Si back bonds generates an unstable $HSi(OH)_3$ molecule over the surface. This unstable molecule, once in solution, decomposes to $Si(OH)_4$ and H_2. In a few cases, $HSi(OH)_3$ molecules or clusters remain on the surface, blocking the corrosion process on selected areas. A summary of the etching process is represented below:

$$SiH_{2_{(surface)}}+3H_2O\rightarrow HSi(OH)_{3_{(surface)}}+2H_2$$

$$HSi(OH)_{3_{(surface)}}\rightarrow HSi(OH)_{3_{(solution)}}$$

$$HSi(OH)_{3_{(solution)}}+H_2O\rightarrow Si(OH)_4+H_2.$$

III. RESULTS

Figure 1 shows AFM images of etched Si(100) surfaces in saturated aqueous ambient for etching times (t) equal to (a) 20 min, (b) 50 min, and (c) 110 min. Figure 1(a) shows the hillocks network across the etched surface; this structure can be associated to a percolation network. When t increases [Fig. 1(b)], the percolation network starts to fracture generating dispersed clusters on the surface. Figure 1(c) shows a transition to globular morphology, with an increase of the mean cluster size.

AFM images of etched Si(111) surface in nonsaturated aqueous ambient are shown in Fig. 2, for t equal to (a) 3 min, (b) 40 min, and (c) 110 min. For small t, the etched Si(111) surface in nonsaturated aqueous ambient (nsa) presents sharp peaks, as shown in Fig. 2(a). Figure 2(b) presents *quasivertical* planes related to the preferential etching rate. Figure 2(c) reveals anisotropic characteristics, with large plateaus dominating the surface.

The growth exponent β is obtained from the time evolution of the surface width saturation value (w_{sat}). Figure 3 shows a log-log plot of w_{sat} vs t. For the same etching time, w_{sat} for Si(100) presents values one order of magnitude greater than for Si(111) surfaces. This increase in the w_{sat} can be attributed to the preferential etching rate.[27] As can be seen in Fig. 3, w_{sat} scales as $w_{sat}\sim t^{\beta}$, with β values for Si(100) and Si(111) in sa, and Si(111) in nsa equal to (0.36 $\pm$0.03), (0.41$\pm$0.02), and (0.44$\pm$0.02), respectively.

Figure 4 shows a log-log plot of HHC vs r, for Si(100) in sa, Si(111) in sa, and Si(111) in nsa. All etched silicon surfaces present self-affine behavior. For large radius a HHC saturation value is attained for all samples, defining a self-affine/saturation region crossover length (C_{sat}).

Etched Si(100) surfaces present self-affine behavior, with α increasing with t from 0.68 to 0.84. With a similar behavior, α evaluated from Si(111) etched in sa rises monotonically with t from $\alpha=0.63$ to $\alpha=0.84$. For short t, the HHC curves for the etched Si(111) surface in nsa present also only one slope, as shown in Fig. 4(c1). When t increases, the HHC curves present two distinct slopes on the self-affine region [Figs. 4(c2) and (c3)]. The presence of two slopes on the self-affine region is a typical of anomalous scaling properties.[23] For short radius, the local interface fluctuations present a local roughness exponent. A local crossover length (C_{local}) defines a transition length between the local and the

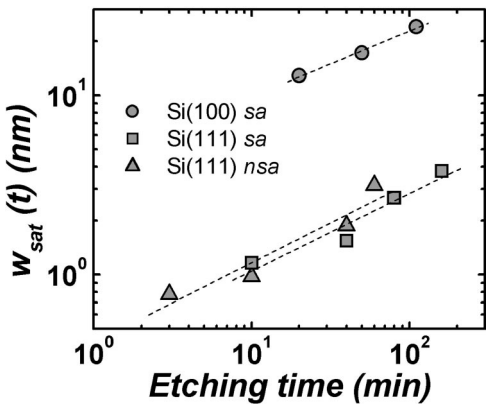

FIG. 3. Surface width saturation vs etching time for: (○) Si(100) in sa, (□) Si(111) in sa and (△) Si(111) in nsa.

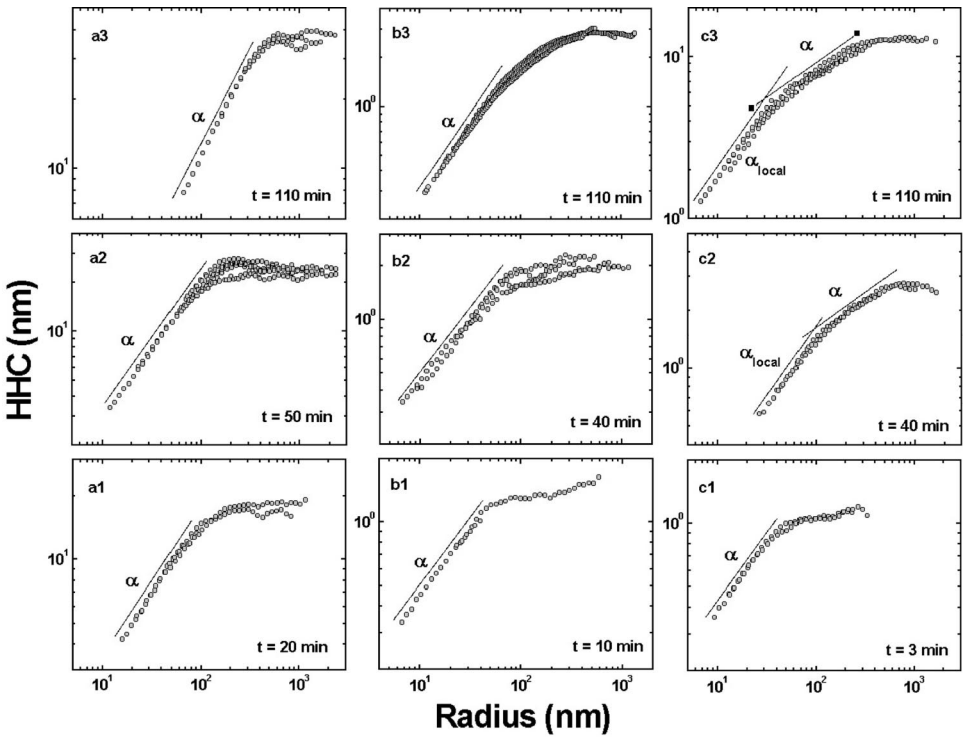

FIG. 4. Height-height correlation function vs radius log-log plots for (a) left column, Si(100) in sa, (b) center column, Si(111) in sa, and (c) right column, Si(111) in nsa. Values are listed in Table I.

global dynamics. This etched Si surface at large times shows a plateau structure [Fig. 2(c)], suggesting that the α_{local} is associated to the plateau growth.

Table I lists critical exponents and crossover lengths values obtained from Figs. 3 and 4. The dynamic exponent Z is estimated by the α/β ratio.

Figure 5 shows a halftone representation of an image of etched Si(100) surface in sa, at $t=50$ min. In order to evidenciate the percolation network, the original image is intersected by a sea plane, generating islands. The sea or threshold level was chosen as 40% of the image maximum height. Figure 6 shows a log-log plot of perimeter (P) vs area (A) for all islands measured at halftone image. Two regions with distinct scaling behaviors were observed at the log-log plot, as is expected for a percolation system.

TABLE I. Experimental values of α, β, Z, and crossovers lengths (C_{local} and C_{sat}) for different experimental conditions. The error associated to α is ± 0.02.

	β	t(min)	α_{local}	α	C_{local} (nm)	C_{sat} (nm)	$Z(\alpha/\beta)$
		20		0.68		114	1.89
Si(100) sa	0.36	50		0.82		128	2.05
		110		0.84		382	2.10
		10		0.63		50	1.54
		40		0.64		70	1.56
Si(111) sa	0.41	80		0.77		167	1.88
		110		0.82		172	2.00
		160		0.84		200	2.05
		3		0.65		46	1.47
		10	0.87	0.45	27	129	1.02
Si(111) nsa	0.44	40	0.72	0.37	104	499	0.84
		60	0.70	0.30	75	660	0.68
		110	0.85	0.42	36	287	0.95

IV. DISCUSSION

A. Percolation in corrosion process

The propagation of high viscosity fluids into a spongelike material is an example of an experimental system with quenched noise.[28] Buldryev *et al.* measured the roughness exponent for the fluid front profiles inside a two-dimensional sponge slice. The measured α is equal to 0.63, and this value suggests a direct percolation process.[28] An unusual example of a percolation system with quenched noise was described by R. Buzio *et al.*[20] at nanostructured sputtered carbon films. These authors proposed that large carbon clusters deposited on the surface may act as a source of quenched noise, suggesting a bi-dimensional percolation system. This assumption is reinforced by the α values measured at these films, close to 0.65.

Figure 1(a) shows a *hillock percolation network* across the image and, for initial etching times of Si(100) in sa, the α values are close to 0.7 (Table I). However, how should one compare the corrosion process with a percolation process? During the Si surface etching the solution plays the role of a fluid; the $HSi(OH)_3$ clusters block the ''fluid invasion,'' similar to the quenched noise, and the resulting surface acts as the fluid invasion front.

Experimental α values at sa ambient increases with the etching time, from ~ 0.6 to ~ 0.8 (Table I). One of the predictions of the KLT model is that the fluid front α value is

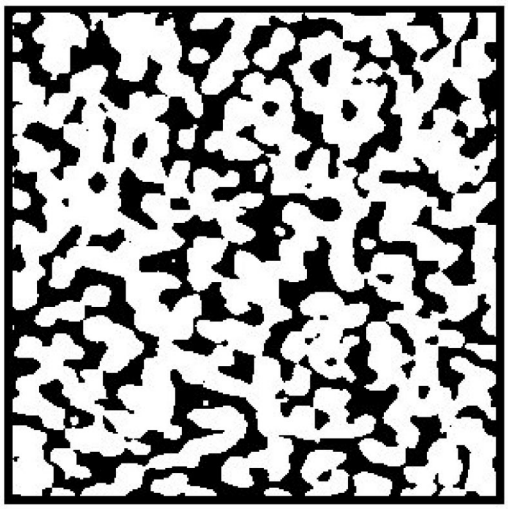

FIG. 5. Percolation islands obtained from a halftone image of etched Si(100) surface, 5 μm$\times$5 μm$\times$121 nm, $t=50$ min.

inversely proportional to the piston velocity, varying from 0.55 (for high effective moving velocity of piston push) to 0.9 (for low ones).[11] To apply the KLT model [Eq. (7)] on corrosion processes, the piston driving force F is associated to the etching rate and the quenched noise $\eta(\vec{x},t)$ is represented by the silicate mask.

The number of etchant ions inside the drop decreases when the etching time increases and consequently the etching power also decreases. This experimental situation is quite similar to that discussed by Gabrielli *et al.*[29] In that work, a *finite volume* of etching solution is in contact with a disordered solid. If the etchant is consumed in the chemical reaction, the process stops spontaneously on a self-similar surface. The dynamics described by Gabrielli *et al.* seems to belong to the universal class of percolation gradient.

Figure 6 shows the perimeter and area scaling relation, $P\sim A^{\phi}$, for Si(100) in sa. This log-log plot presents two slopes, one for large areas and the other for small areas, with $\phi=1$ and for $\phi=1/2$, respectively.

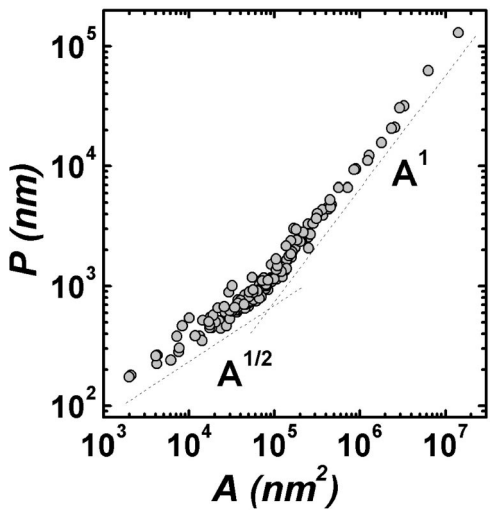

FIG. 6. Perimeter vs area log-log plot for islands obtained from Fig. 5.

Nonpercolated or isolated islands show a globular characteristic, and consequently ϕ is close to 1/2. On the other hand, percolated structures present $\phi\simeq 1$, related to the high perimeter/area ratio for ''large percolated archipelagos.''[19]

B. Local and global self-affine behavior

Recently López[23] proposed an analytical approach to predict when a particular growth model is expected to have anomalous properties, i.e., to give two independent and distinct roughness exponents. The *local* roughness exponent characterizes the surface fluctuations at small distances. The existence of *local* and *global* behavior can also be found in organic films,[30] annealed $LiCoO_2$ films,[16] Al films,[31] mountains topographic profiles,[32] and Ni evaporated thin films.[33] For the Ni evaporated films, the experimental results suggest a local diffusional behavior and a global KPZ behavior.[33]

Height-height correlation function for Si(111) surfaces in nonsaturated aqueous ambient [Figs. 4(c2) and (c3)] presents anomalous scaling behavior. Figure 2(c) shows the AFM micrograph corresponding to the plot shown in Fig. 4(c3), with plateau structures at the surface. For short correlation radius analysis (α_{local}), the HHC describes the dynamic associated to the *local* correlations, i.e., the correlations on the plateaus. For $t=110$ min, α_{local} is equal to 0.85, lower than the theoretical expected $\alpha=1$ for a diffusional process, described by the WV model[21] [Eq. (4)]. The underestimated α_{local} value can be related to the plateau edges effect: when the HHC circle center is close to the facet edge, the height difference changes abruptly, causing a decrease in the α (mean) value [see Eq. (1)].

The ensemble of plateaus suggests a preferential growth direction, and surfaces with preferential growth direction are generally described by the KPZ model[25] [Eq. (6)]. The α global values are consistent, within experimental errors, with the KPZ theory of surface growth ($\alpha\approx 0.39$).

C. Growth and dynamic exponents

Completely uncorrelated surfaces (such as in random deposition) present growth exponent β equal to 0.5, and for various continuous growth models[6,21,25] β is equal to 1/4. Experimental β values for etched Si surfaces obtained from the data in Fig. 3 are $\beta\approx 0.36$ for Si(100) and $\beta\approx 0.42$ for Si(111), suggesting that the corrosion process can be described by a weakly correlated model.

Studying interface growth at medium with pinning forces, Leschhorn estimated $\beta\sim 0.47$.[34] Leschhorn's model was simulated by Jost and Usadel in $(2d+1)$ using a cellular automata. They obtained the critical exponents $\alpha=2/3$ and $\beta=4/9$.[35] Experimental exponents values (our work) for Si(111) are $0.63<\alpha<0.84$ and $\beta\approx 0.42$, suggesting that the corrosion process is in the same universality class of viscous medium with quenched noise.

One of the possible ways to measure the correlation length parallel to the surface ($\xi_{\parallel}$) is the saturation crossover length C_{sat}. The dynamic exponent Z_{scl} can be estimated from the scaling relation $C_{sat}\sim t^{1/Z_{scl}}$. Z can also be obtained from the α/β ratio, and this value is a function of the correlation length vertical to the surface, $\xi_{\perp}$. For the initial etch-

ing stages of Si(111) in nsa ($t \leqslant 60$ min) the calculated dynamic exponent values are $Z_{scl} = 1.10 \pm 0.05$ and $Z = 1.00 \pm 0.34$. The agreement between these two dynamic exponent values, obtained from correlation lengths parallel or vertical to the surface, corroborate the possibility to describe the etched surface such as a self-affine surface.

V. CONCLUSIONS

A self-affine behavior has been characterized for etched Si surfaces. Experimental growth exponents values are lower for Si(100) ($\beta \cong 0.36$) than for Si(111) ($\beta \sim 0.4$). These β values suggest a weakly correlated surface.

For etched Si surfaces in sa the roughness exponent value increases with etching time from ~ 0.6 to ~ 0.8. The α functional behavior with etching time can be qualitatively described by the KLT percolation model.

Etched Si(111) surfaces in nsa present anomalous scaling behavior with $\alpha_{local} \sim 2/3$ and $\alpha_{global} \sim 0.4$. Local correlations were associated to the plateau's growth, and global correlations to the preferential growth direction described by KPZ model. These results suggest that the etching process belongs to the same universality class of viscous medium with quenched noise.

ACKNOWLEDGMENTS

We are grateful to L. O. Bonugli and J. R. Castro for technical assistance, to A. Gorenstein for helpful discussions, and acknowledge financial support from CNPq Grant Nos. 523.268/95-5, 140302/00-0 and FAPESP 98/14769-2.

*Electronic address: kleinke@ifi.unicamp.br

[1] W. Kern, J. Electrochem. Soc. **137**, 1887 (1990).
[2] J. Kasparian, M. Elwenspoek, and Philippe Allongue, Surf. Sci. **388**, 50 (1997).
[3] J. M. Williams and T. P. Beebe, Jr., J. Phys. Chem. **97**, 6249 (1993); **97**, 6255 (1993).
[4] H.-A. Durand, K. Sekine, K. Etoh, K. Ito, and I. Kataoka, J. Appl. Phys. **84**, 2591 (1998).
[5] V. W. Stone, A. M. Jonas, B. Nysten, and R. Legras, Phys. Rev. B **60**, 5883 (1999).
[6] J. Krim and G. Palasantzas, Int. J. Mod. Phys. B **9**, 599 (1995).
[7] S. B. Santra and B. Sapoval, Physica A **266**, 160 (1999).
[8] R. Cafieiro, V. Loretto, and P. P. Prosini, Europhys. Lett. **42**, 389 (1998).
[9] L. E. Scriven and C. V. Sternling, Nature (London) **187**, 186 (1960).
[10] M. E. R. Dotto and M. U. Kleinke, Physica A **295**, 149 (2001).
[11] D. A. Kessler, H. Levine, and Y. Tu, Phys. Rev. A **43**, 4551 (1991).
[12] M. U. Kleinke, O. Teschke, and M. A. Tenan, J. Electrochem. Soc. **138**, 2763 (1991).
[13] M. U. Kleinke, O. Teschke, and M. A. Tenan J. Electroanal. Chem. **344**, 107 (1993).
[14] A.-L. Barabási and H. E. Stanley, *Fractal Concepts in Surface Growth* (Cambridge University Press, Cambridge, England, 1995).
[15] F. Family, Physica A **168**, 561 (1990).
[16] M. U. Kleinke, J. Davalos, C. Polo da Fonseca, and A. Gorenstein, Appl. Phys. Lett. **74**, 1683 (1999).
[17] R. F. Voss, R. B. Laibowitz, and E. I. Alessandrini, Phys. Rev. Lett. **49**, 1441 (1982).
[18] A. Kapitulnik and G. Deutscher, Phys. Rev. Lett. **49**, 1444 (1982).
[19] R. Viswanathan and M. B. Heaney, Phys. Rev. Lett. **75**, 4433 (1995).
[20] R. Buzio, E. Gnecco, C. Boragno, U. Valbusa, P. Piseri, E. Barborini, and P. Milani, Surf. Sci. **444**, L1 (2000).
[21] D. Wolf and J. Villain, Europhys. Lett. **13**, 389 (1990); J. Villain, J. Phys. I **1**, 19 (1991).
[22] Z. W. Lai and S. Das Sarma, Phys. Rev. Lett. **66**, 2348 (1991).
[23] J. M. López, Phys. Rev. Lett. **83**, 4594 (1999).
[24] J. Krug, Phys. Rev. Lett. **72**, 2907 (1994).
[25] M. Kardar, G. Parisi, and Y. C. Zhang, Phys. Rev. Lett. **56**, 889 (1986).
[26] J. Rappich, H. J. Lewerenz, and H. Gerischer, J. Electrochem. Soc. **140**, L187 (1993).
[27] H. E. Hessel, A. Feltz, M. Reiter, U. Memmert, and R. J. Behm, Chem. Phys. Lett. **186**, 275 (1991).
[28] S. V. Buldyrev, A.-L. Barabási, F. Caserta, S. Havlin, H. E. Stanley, and T. Vicsek, Phys. Rev. A **45**, R8313 (1992).
[29] A. Gabrielli, A. Baldassarri, and B. Sapoval, Phys. Rev. E **62**, 3103 (2000).
[30] F. Biscarini, P. Samori, O. Greco, and R. Zamboni, Phys. Rev. Lett. **78**, 2389 (1997).
[31] A. E. Lita and J. E. Sanchez, Phys. Rev. B **61**, 7692 (2000).
[32] M. Matsuchita and S. Ouchi, Physica D **38**, 246 (1989).
[33] Z. Csahok, Z. Farkas, M. Menyhard, G. Gergely, Cs. S. Daroczi, Surf. Sci. **364**, L600 (1996).
[34] H. Leschhorn, Physica A **195**, 324 (1993).
[35] M. Jost and K. D. Usadel, Physica A **255**, 12 (1997).